Geothermics 83 (2020) 101710

Contents lists available at ScienceDirect

Geothermics

journal homepage: www.elsevier.com/locate/geothermics

Comparative performance analysis of building foundation Ground heat exchanger

Nurullah Kayaci[a,*], Hakan Demir[b]

[a] Department of Mechanical Engineering, Namık Kemal University, Çorlu, 59860, Tekirdağ, Turkey
[b] Department of Mechanical Engineering, Yıldız Technical University, Besiktas, 34349, Istanbul, Turkey

ARTICLE INFO

Keywords:
Ground source heat pump
Building foundation
COP
Optimization
Economic analysis

ABSTRACT

The aim of this work is to improve the performance of Ground-Source Heat Pumps (GSHPs) by placing the heat exchanger pipes in the soil under the building foundation and in the building foundation reconstructed in Turkey. In this scope, firstly, experimental studies have been performed on horizontal parallel pipes buried in soil under the foundation of the 2400 m^2 Central Laboratory building, which was newly built at Yıldız Technical University. A comparison between the results of the experimental and newly developed numerical model is presented. Then, a full-scale numerical model for a shopping mall is developed based on the pipe location (soil and concrete layer), Numbers of Parallel Tube (NPTs) and different condensation temperatures in the heating season. The results show that the COP of GSHP when the pipes are buried in the soil under the building foundation is greater than when the pipes are buried in the building foundation. Furthermore, considering capital investment and operational costs, a reference function is defined as an optimization parameter. The effects of the pipe location, increasing rates in electricity prices and NPTs on reference function are investigated. For higher NPT values, locating the pipes in the foundation gives higher values of the reference function while for lower NPT values it is vice versa.

1. Introduction

In the west of Turkey, particularly in and around Istanbul, buildings are reconstructed rapidly with state support due to the earthquake risks. As it is obligatory to acquire an energy performance certificate for the buildings, renewable energy sources have started to be in demand. The subsidization of low-carbon houses and workplaces by the state has got the consumers to prefer renewable energy sources. GSHP and solar energy systems are favored notably in large-scale buildings, such as shopping malls or state buildings. Thus, Turkey is devoting significant efforts about energy diversity by using renewable energy sources in order to diminish its energy dependence and increase the utilization of local resources (Lund and Boyd, 2015).

ASHRAE (ASHRAE Geothermal heating and cooling, 2014) essentially classifies geothermal energy resources into three categories: (i) high-temperature (> 150 °C) for electric power production, (ii) intermediate- and low-temperature (< 150 °C) for direct-use applications, and (iii) GSHP applications (< 32 °C). GSHP systems have attracted intensive attention in recent decades as an alternative energy source for residential and commercial space heating and cooling applications.

Many studies have been carried out analytically, numerically or experimentally to obtain the temperature distribution in the soil. There are basically two types of analytical approaches in literature. The first of these is the Kelvin Line Source Theory and the other is the Cylinder Source Theory. Only the symmetrical soil temperature distribution around the pipe can be obtained by using these source theories (Gu and O'Neal, 1995; Hastaoglu et al., 1995; Lei, 1993; Mukerji et al., 1997; Negiz et al., 1993, 1995; Chiasson, 1999; Mei, 1991). In the analytical model proposed by Metz (1983), the temperature distribution in the soil was obtained by dividing the soil into blocks around the coil by making some changes in the Line Source theory. However, two or three-dimensional steady-state and time-dependent temperature distribution in the soil can only be solved using numerical techniques.

In Demir et al. (2009) is developed a model to solve the unsteady-three dimensional heat conduction equations with the surface effects and real meteorological data in soil. The model written in MATLAB was compared with the experimental studies carried out at Yildiz Technical University and found to be in good agreement with each other. Kayaci and Demir developed (Kayaci and Demir, 2018a) a new model to obtain transient soil temperature distribution for horizontal Ground Heat Exchanger (GHE) for ten year period. In addition to this study, the long time performance analysis of GSHP for space heating and cooling

* Corresponding Author.
E-mail address: nkayaci@nku.edu.tr (N. Kayaci).

https://doi.org/10.1016/j.geothermics.2019.101710
Received 5 July 2018; Received in revised form 12 May 2019; Accepted 2 August 2019

Nomenclature

A	Total annual payment (ncu)
C_i	Capital investment (ncu)
C_{pipe}	Pipe cost (ncu)
$C_{earthwork}$	Earthwork cost (ncu)
$C_{heatpump}$	Heat pump cost (ncu)
$C_{circpump}$	Circulation pump cost (ncu)
C_{labor}	Labor cost (ncu)
C_e	Operational costs (ncu)
e	Increasing rate in electricity prices
E_{tariff}	The tariff of unit electricity consumption of workplaces (ncu/kWh)
E_{pump}	The total electricity consumption of the circulating pump (kWh)
E_{comp}	The total electricity consumption of the compressor (kWh)
F_{ref}	Reference function (kW/ncu)
H	Simulation depth (m)
k_f	Thermal conductivity of fluid (W/m K)
k_s	Thermal conductivity of soil (W/m K)
k_c	Thermal conductivity of concrete (W/m K)
L	Pipe length (m)
P_s	Pipe spacing (m)
$\dot{q}_h$	Heat flux due to convective heat transfer (W/m^2)
T_a	Air temperature (K)
$T_{a,h}$	Indoor air temperature in heating season (°C)
$T_{a,c}$	Indoor air temperature in cooling season (°C)
$T_{f,i}$	Fluid inlet temperature (°C)
$T_{f,o}$	Fluid outlet temperature (°C)
T_i	Initial temperature (°C)
T_s	Soil temperature (°C)
$T_{s,a}$	Amplitude of soil temperature (°C)
$T_{s,m}$	Average temperature of soil surface (°C)
T_y	Surface temperature (K)
V_f	Flow rate (m^3/h)
Y	Burial depth (m)
Y_c	Foundation height (m)

Greek Letters

α_t	Thermal diffusivity of soil (m^2/h)
τ_h	Running time in the heating season (hours)
τ_c	Running time in the cooling season (hours)

applications based on thermo-economic optimization criteria is executed (Kayaci and Demir, 2018b).

Nam and Chae (2014) suggested the method for the prediction of the ground Heat Exchange Rate (HER) to determine the optimum design tools of an energy-foundation for a horizontal heat exchanger. The simulation model that links the models with ground heat transfer, ground surface heat and GHE was developed. The many case studies on predication of HER were carried out at different conditions of the GHE design such as the pipe spacing, burial depth, volumetric flow rate, pipe diameter, and operation condition.

Moon and Choi (2015) carried out the heating performance analysis of a GSHP system using energy-pile and energy-slab Ground Loop Heat Exchangers (GLHXs) experimentally. This experimental system decreases the construction cost of the GLHXs since it does not need additional area and boring for installation of GLHXs. 150 building structural energy-piles of GLHX with a length of 13.8 m from the bottom of the basement floor and 10 energy-slab GLHX with a length of 180 m were installed. The results showed that the minimum COPs of the heat pump unit for the energy-pile and energy-slab systems were 4.2 and 4.5, respectively.

The aim of this work is to improve the performance of GSHPs by placing horizontal GLHX in the soil under the building foundation and in building foundation reconstructed in Turkey, by which not only will the most important obstacle in the applications of GSHP, namely earthwork costs will be eliminated or diminished but also houses and workplaces with low-carbon emissions will be acquired. In this scope, firstly, experimental studies have been performed on horizontal GLHX pipes buried in soil under the foundation of the 2400 m^2 newly Central Laboratory building established at Yıldız Technical University, the newly developed numerical model is validated with experimental results. Then, a full scale numerical model for a shopping mall is developed based on the installation place of the pipes, and NPTs. The mall is conditioned from 9 a.m. till 10 pm all the year round. At this time interval for each day during heating and cooling seasons, a continuous 20 kW of total heating/cooling load of shopping mall is extracted/transferred from/to the soil or concrete. Thanks to the code written in MATLAB environment, the effects of installation place of the pipes and NPT are analyzed in the case studies.

The hourly fluid inlet and outlet temperature in the pipe, soil and concrete temperatures vicinity of the pipe are obtained in ten years by conducting case studies. By means of a new code developed in MATLAB, these temperatures are given as input parameters and then the energy analysis is performed in the heat pump cycle. This procedure is carried out for 3 different condensation temperatures in the heating season. As a result of these optimization studies, many different case studies are achieved.

By performing the energy analysis for all case studies, hourly COP values for ten years are calculated. The electricity consumption of compressor is determined by dividing the certain heating and cooling loads provided to shopping mall into the hourly calculated COP values. The electricity consumption of the circulation pumps during the running time is also calculated. The total electricity consumption of the system is calculated on an hourly basis and then operational costs are obtained. According to the Energy Regulators Regional Association (ERRA) of Turkey, the electricity prices for workplaces have gone up 11% in the last decade. This is called the increasing rate in electricity prices and it is included in all case studies. Besides the operational costs of GSHP systems, the capital investment costs are as follows: pipe cost, earthwork cost, heat pump cost, circulation pump cost and labor cost. Considering capital investment and operational costs, a reference function is defined as an optimization parameter. The reference function is determined by dividing the total annual heating and cooling loads provided to shopping mall into the total annual payment. It is obtained for the all case studies.

The novelty of this work, although the GSHP systems are well-known method, its applied engineering costs like excavation costs make them infeasible for the economic aspects. Also, the additional land requirements of the GSHPs bring another challenge for the real-scale engineering studies. Thus, we proposed a new method to bury the GHEs into the building foundation layers (two layers are studied in this study as the soil and concrete layers), therefore, it is eliminated or diminished the excavation costs. To investigate the thermal performance of new method in the building foundation, experimental studies with the real-scale (2400 m^2 area) GSHP systems is conducted. Also, a unique numerical modeling, which includes conductive and convective heat transfer phenomena, is validated with the experimental outputs for the further developments.

2. Experimental study

Experimental setup was applied to the newly built Central Laboratory building at Yıldız Technical University, Davutpaşa Campus

(Kayaci et al., 2019). After excavation, the GLHX pipes were placed in the soil under the building foundation and covered with sand (Fig. 1a and b).

The GLHX pipes placed in the soil under the building foundation is included of 10 parallel pipes with a length of 85 m. The distance between pipes is 0.5 m. Following the GLHX pipes were buried in the soil, the lean concrete was poured (Fig. 1c). The final appearance of the Central Laboratory building is given in Fig. 1d. The GLHX pipes were connected to the collector and taken into the building, and then integrated to the heat pump. The view of the heat pump is shown in Fig. 2. The technical characteristics of all installation components on the heat pump are given in Table 1.

Within the scope of experiments, in the continuous operation of the system, that is, when the living space needs the heating load, the results of experimental and simulation are fairly compatible with each other. However, when the living space does not need the heating load, the heat extracted from the Ground layer continues until the temperature of the accumulation tank, integrated into the heat pump, reaches the operation temperature, and the heat pump switches itself off.

For the measurement system in experiments, the water inlet and outlet temperatures of the GLHX pipes were measured using Resistance Temperature Detectors (RTDs), and the flow rate was measured using a turbine-type flow meter. The data obtained from RTD and flow meter were recorded by connecting to Programmable Logic Controller (PLC) as is indicated in Fig. 3a.

Ceiling cassette fan-coil unit is used for occupied space, is depicted in Fig. 3b. Ceiling cassette fan-coil unit provide each served space an independent controlled temperature zone to suit many different requirements.

3. Model development

A new model with realistic boundary conditions is developed to solve the unsteady-three dimensional temperature distribution around the pipes placed in soil and concrete. The temperature gradient along the pipe axis is negligible as it is very small. Thus, the heat transfer equations in soil and concrete are solved in dynamic boundary conditions and two-dimensional geometry by including the water temperature in the domain. Firstly, the governing Eq. (1) is solved for the all domain in two-dimensions and the solution is then expanded along pipe's length to obtain the solution in three dimensions.

Fig. 2. The components of heat pump.

$$\frac{\partial^2 T(x, y, t)}{\partial x^2} + \frac{\partial^2 T(x, y, t)}{\partial y^2} = \frac{1}{\alpha}\frac{\partial T(x, y, t)}{\partial t} \quad (1)$$

where α is the thermal diffusivity of the medium through which heat travels. Some assumptions about the developed model were described previously (Kayaci and Demir, 2018a). The details were given in the study.

The parallel pipe horizontal GLHX and solution area in soil and concrete are indicated in Fig. 4a and b, respectively. The model consists

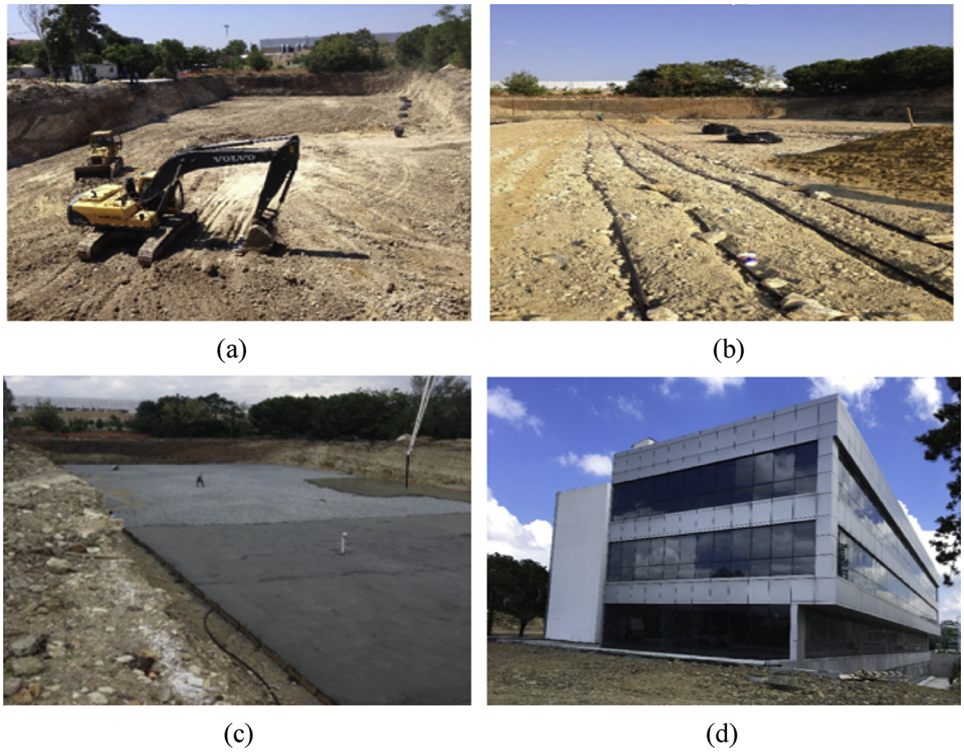

Fig. 1. Experimental setup: (a) Work-in progress excavation works, (b) placement of the pipes, (c) implementation of lean-concrete layer, (d) Central Laboratory building.

Table 1
The technical characteristics of all installation components.

Element	Technical Specification
1-Ground Source Heat Pump	Manufacturer: Restherma; Type: IP11SS **Heating**: Nominal capacity: 10.5 kW, Power:2.1 kW, COP:5, Operating temp. range:-5/ + 45 °C,Max. outlet water temp.: 55 °C **Cooling**: Nominal Capacity: 8.5 kW, Power:1.98 kW, EER:4.29 Operating temp. range: + 10/ + 43 °C, Max. outlet water temp.: + 7 °C
2-Flow Switch	Manufacturer: Ayvaz, Type: AK 100, Diameter:16mm
3-Pumps	a-) Manufacturer: Grundfos, Type: MAGNA-3 25-100 Max. flow rate: 78.5 m^3/h, Max. Head: 18 m, Max. System pressure: 16 bar Liquid temp.: -10 to 110 °C b-) and c-) Manufacturer: Grundfos, Type : Alpha-2 25-80 180 Max. flow rate: 4.8 m^3/h, Max. Head: 5.8 m, Max. System pressure: 10 bar, Liquid temp.: 2 to 110 °C
4-Accumulation Tank	Manufacturer: Resboyler, Type: KAT Capacity: 100lt, Test pressure: 13kg/cm^2, Operating pressure: 10 kg/cm^2
5-Thermometer	Manufacturer: Pakkens, Type: TE100DB1 Measurement range: -30/ + 60 °C, Temp. element: Bi-metal
6-Manometer	Manufacturer: Pakkens, Type: MG063DRM1 Measurement range: 0-10 bar/0-120 psi
7-Dirt Separator	Manufacturer: Reflex, Type: Exdirt Max. operating temp. 110 °C, Max. operating pressure: 10 bar
8-Air Separator	Manufacturer: Reflex, Type: Exvoid T Max. operating temp. 110 °C, Max. operating pressure: 10 bar
9-Balance Tank	Manufacturer: Reflex, Type: 15P1125 Allowable working temperature/flow temp: -10/120 °C Max. working temp., diaphragm: -10/70 °C, Precharge press: 1,5 bar, Allowable work. pressure: 6 bar, Volume: 23L
10-RTD	Manufacturer: Tekon, Type: PT100, Measurement range: 0/100 °C
11-Flow Meter	Manufacturer: Bass, Type: FMPV Range: 0-6 m^3/h, Temperature: -10/70 °C, Pressure: 10 bar max.

of horizontal parallel pipes of length L and pipe spacing of P_s. As depicted in Fig. 4a, if the pipe is buried in the soil, Y is the depth of the buried pipe, Y_c is the height of the building foundation and Y-Y_c is the depth buried in the soil. As depicted in Fig. 4b, if the pipe is buried in the concrete, Y is the depth of the buried pipe, Y_c is the depth of the building foundation.

Initial and boundary conditions of problem for solution domain are defined as below;

$$T_i = T(y, t), \ t = 0 \tag{2}$$

$$\left.\frac{\partial T}{\partial x}\right|_{x=P_s/2} = 0 \tag{3}$$

$$\left.\frac{\partial T}{\partial x}\right|_{x=0} = 0 \tag{4}$$

$$q(W/m^2), y = H \tag{5}$$

$$q_t(W/m^2), \ y = 0 \tag{6}$$

Initial temperature distribution of the soil profile is obtained as follows (Kasuda and Archenbach, 1965):

$$T(y, t) = T_{s,m} + T_{s,a} e^{-y\sqrt{\frac{\pi}{\alpha_s P}}} \cos\left(2\pi\frac{t}{P} - y\sqrt{\frac{\pi}{\alpha_s P}}\right), \ t = 0, \ x = x, 0 < y < H \tag{7}$$

This equation is only used to determine the unaffected soil temperature (at the beginning of the simulation time). The change of heat transfer inside the pipe is indicated in Fig. 5.

Variation of fluid temperature inside the pipe can be written by using energy conservation as below;

$$T_{f,o} - T_{f,i} = \frac{q}{m_f Cp_f} l \Rightarrow dT_{f,oi} = \frac{q}{m_f Cp_f} dl \tag{8}$$

Due to the difference between the soil temperature and the fluid temperature, the heat transfer occurs. That is, decrease in soil temperature induces the increase in fluid temperature.

$$T = T_s - T_f \Rightarrow dT = dT_{f,oi} \tag{9}$$

The amount of heat transferred from the unit pipe length is;

$$q = k_s(T_s - T_f)F(z) = k_s TF(z) \tag{10}$$

Eq. (8) and (10) are combined and rewritten as;

$$\frac{k_s TF(z)}{mCp_f} dl = -dT \tag{11}$$

(a) (b)

Fig. 3. The views of (a) PLC system and (b) Ceiling cassette fan-coil unit.

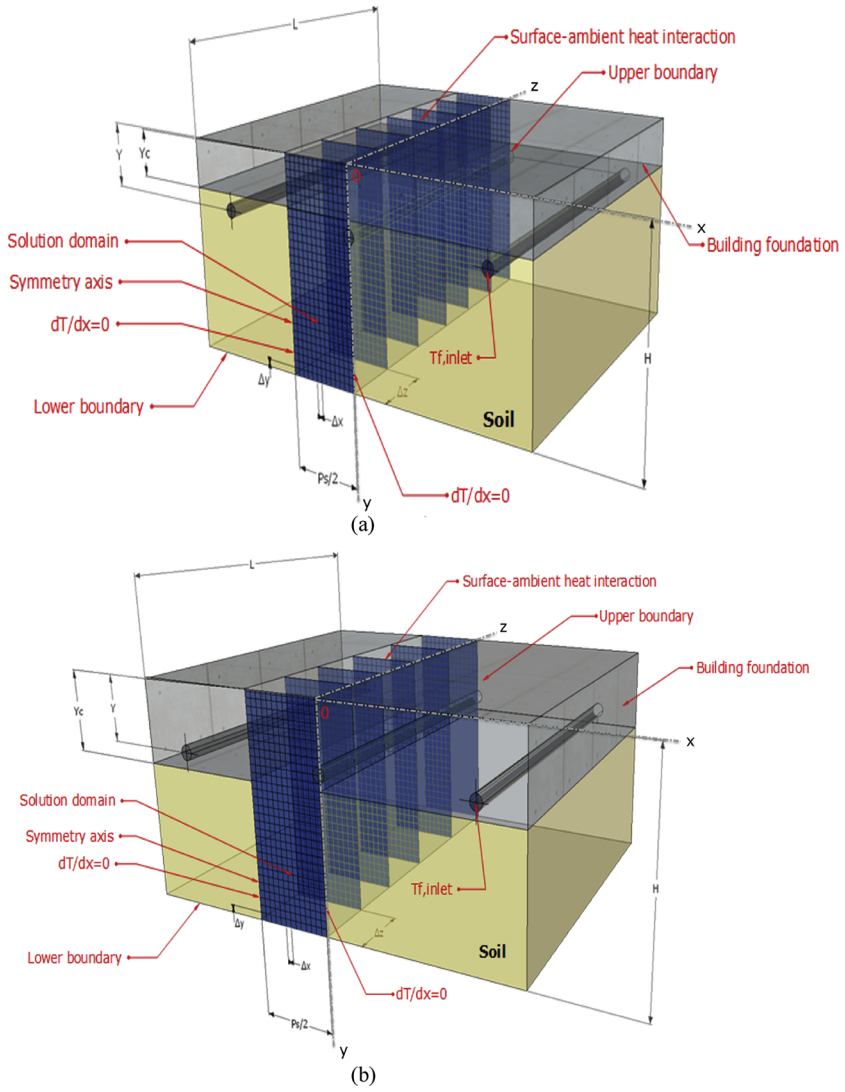

Fig. 4. The pipes buried (a) in the soil under the building foundation, (b) in the building foundation and solution domains.

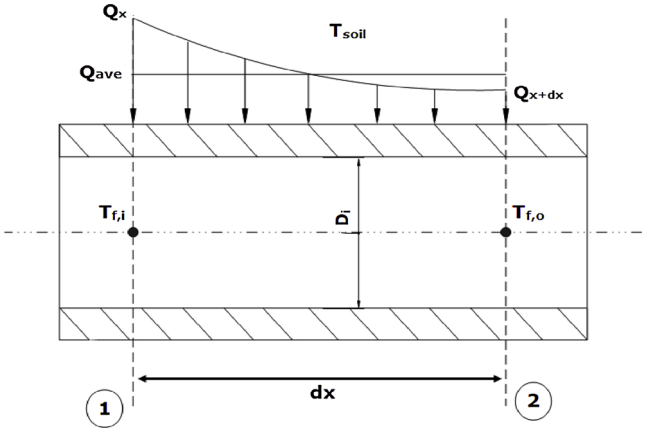

Fig. 5. Variation of heat transfer inside the pipe.

This equation is integrated and the fluid outlet temperatures are calculated as below;

$$\int_{T_{f,i}}^{T_{f,o}} -\frac{dT}{T} = \frac{k_s F(z)}{mCp_f} \int_0^L dl \tag{12}$$

$$T_{f,o} = T_s - (T_s - T_{f,i}) e^{\frac{k_s F(z) L}{mCp_f}} \tag{13}$$

$$z = \frac{\alpha t}{r^2} \tag{14}$$

$$F(z) = \frac{8}{\pi} \int_0^\infty \frac{e^{-z\beta^2}}{J_0^2(\beta) + Y_0^2(\beta)} \frac{d\beta}{\beta} \tag{15}$$

F (z) predicts a decrease in the heat transferred from/to the soil due to the useless of the soil over time. Eq. (16) is obtained as follows, if the expression F (z) is not taken into account in Eq. (13).

$$T_{f,o} = T_s - (T_s - T_{f,i}) e^{\frac{-k_s L}{m_f C_{p,f}}} \tag{16}$$

where $T_{f,i}$ is the fluid inlet temperature, $T_{f,o}$ is the fluid outlet temperature, T_s is the soil temperature, and k_s is the soil thermal conductivity. m_f is the mass flow rate and $C_{p,f}$ is the specific heat of water.

Similarly, when the pipe is buried in the concrete, the fluid outlet temperatures are calculated by using the energy balance between the pipe and solution domain in concrete as below;

$$T_{f,o} = T_c - (T_c - T_{f,i}) e^{\frac{-k_c L}{m_f C_{p,f}}} \tag{17}$$

where T_c is the concrete temperature, and k_c is the concrete thermal conductivity.

The temperature distribution of the fluid along the pipe is evaluated and applied by linking it to the two-dimensional solution domains. The soil and concrete temperature profiles in three dimensions might be determined by separating the whole pipe into small parts in order to calculate the fluid inlet and outlet temperatures by using the fluid outlet temperatures as fluid inlet temperature of the next part.

The equations of heat transfer in the soil and concrete with Alternating Direction Implicit (ADI) method are used to obtain the nodal temperatures by writing the difference formulas separately for rows and columns in two consequent time steps. Eq. (1) is solved using ADI method (Ling and Zhang, 2004; Mihalakakou, 2002). The finite difference form of Eq. (1) at $(n+1)^{th}$ time is;

$$\frac{T_{i,j}^{n+1} - T_{i,j}^{n}}{\alpha.\,\Delta t} = \frac{T_{i-1,j}^{n+1} - 2.T_{i,j}^{n+1} + T_{i+1,j}^{n+1}}{(\Delta x)^2} + \frac{T_{i,j-1}^{n} - 2.T_{i,j}^{n} + T_{i,j+1}^{n}}{(\Delta y)^2} \tag{18}$$

and at $(n+2)^{th}$ time;

$$\frac{T_{i,j}^{n+2} - T_{i,j}^{n+1}}{\alpha.\,\Delta t} = \frac{T_{i-1,j}^{n+1} - 2.T_{i,j}^{n+1} + T_{i+1,j}^{n+1}}{(\Delta x)^2} + \frac{T_{i,j-1}^{n+2} - 2.T_{i,j}^{n+2} + T_{i,j+1}^{n+2}}{(\Delta y)^2} \tag{19}$$

for equal spacing in x and y directions

$$\Delta x = \Delta y, \frac{\alpha.\,\Delta t}{(\Delta x)^2} = \frac{\alpha.\,\Delta t}{(\Delta y)^2} = r \tag{20}$$

These formulas are rearranged to perform the unknown and known of each time step on the right and left hand side, respectively, as below;

$$-r.\,T_{i-1,j}^{n+1} + (1+2r).\,T_{i,j}^{n+1} - r.\,T_{i+1,j}^{n+1} = r.\,T_{i,j-1}^{n} + (1-2r).\,T_{i,j}^{n} + r.\,T_{i,j+1}^{n} \tag{21}$$

$$-r.\,T_{i,j-1}^{n+2} + (1+2r).\,T_{i,j}^{n+2} - r.\,T_{i,j+1}^{n+2} = r.\,T_{i-1,j}^{n+1} + (1-2r).\,T_{i,j}^{n+1} + r.\,T_{i+1,j}^{n+1} \tag{22}$$

The energy balance on the interfacial nodes of the concrete and soil is written for the control volume around each node. Fig. 6 shows the energy balance for a node on the layer interface between the concrete and soil by considering the control volume around the node and the heat fluxes.

The energy balance obtained is given in Eq. 23 (Rezaei et al., 2012):

$$q_1 - q_3 + q_3 - q_4 = (\rho C_p)_{ave}(\Delta x)(\Delta y)\frac{\partial T_{i,j}}{\partial t} \tag{23}$$

where;

$$(\rho C_p)_{ave} = \frac{(\rho C_p)_{soil} + (\rho C_p)_{concrete}}{2},\ k_{ave} = \frac{k_s + k_c}{2} \tag{24}$$

and the terms of heat fluxes are:

$$q_1 = k_{ave}\frac{T_{i-1,j}^{n} - T_{i,j}^{n}}{\Delta x}\Delta y \tag{25}$$

$$q_2 = k_{ave}\frac{T_{i+1,j}^{n} - T_{i,j}^{n}}{\Delta x}\Delta y \tag{26}$$

$$q_3 = k_c\frac{T_{i,j-1}^{n} - T_{i,j}^{n}}{\Delta y}\Delta x \tag{27}$$

$$q_4 = k_s\frac{T_{i,j+1}^{n} - T_{i,j}^{n}}{\Delta y}\Delta x \tag{28}$$

Replacing all the heat flux equations into the energy balance equation and rearranging the equations provide the new parameters in the difference equation as defined below.

$$r_{ave} = \frac{k_{ave}}{(\rho C_p)_{ave}}\frac{\Delta t}{(\Delta x)^2} \tag{29}$$

$$r_c = \frac{k_c}{(\rho C_p)_{ave}}\frac{\Delta t}{(\Delta x)^2} \tag{30}$$

$$r_s = \frac{k_s}{(\rho C_p)_{ave}}\frac{\Delta t}{(\Delta x)^2} \tag{31}$$

The difference formulas of the ADI method are reconsidered and new difference formulas for top and bottom interfacial nodes of soil and concrete layer are obtained. Eq. (32) and (33) are new interfacial formulas for rows (x-smoothing) and columns (y-smoothing), respectively (Rezaei et al., 2012).

$$-r_{ave}.\,T_{i-1,j}^{n+1} + (1+2r_{ave}).\,T_{i,j}^{n+1} - r_{ave}.\,T_{i+1,j}^{n+1} = r_s.\,T_{i,j-1}^{n} + (1-r_s-r_c).\,T_{i,j}^{n} + r_c.\,T_{i,j+1}^{n} \tag{32}$$

$$-r_s.\,T_{i,j-1}^{n+2} + (1+r_s+r_c).\,T_{i,j}^{n+2} - r_c.\,T_{i,j+1}^{n+2} = r_{ave}.\,T_{i-1,j}^{n+1} + (1-2r_{ave}).\,T_{i,j}^{n+1} + r_{ave}.\,T_{i+1,j}^{n+1} \tag{33}$$

Since the upper surface of the building foundation is a covered area, convection and long wave radiation heat transfer occur on the upper surface of the building foundation. By using energy balance equations, the surface heat flux is performed by considering the mechanisms of surface-ambient heat interaction. The equation of the heat flux due to the convection and long wave radiation on the upper surface of the building foundation is given below:

$$\dot{q}_h = h_{combined}(T_a - T_y) \tag{34}$$

where $h_{combined}$ (W/m^2 K) is the combined heat transfer coefficient of air. T_a (K) is the indoor air temperature above building foundation and T_y (K) is the surface temperature on the upper surface of building foundation.

By using the equations of ADI finite difference, the temperature distribution of soil and concrete are solved consecutively at a given time (Von Rosenberg, 1969). Thomas Algorithm can be applied to solve the equations as the resulting matrixes are tri-diagonal. Therefore, the equations of ADI finite difference are solved together with the boundary conditions in MATLAB environment and the consequences of solution parameters on the results are analyzed. Block diagram of solution algorithm is created as indicated in Fig. 7. The details of block diagram about the developed model were expressed previously.

The new developed model, written in MATLAB, can be used in the engineering applications of GSHP to simulate the three dimensional thermal behavior of the fluid inside Ground and Concrete layers. Two different GLHX (the pipes buried in soil and concrete) with a pipe diameter of 0.026 m, a pipe length of 85 m and a simulation depth of 20 m are quite difficult to generate mesh in commercial programs. Also, while the finite volume method for solution is used in these programs, the finite difference method is used in the developed model. In addition to this, some UDFs must be written to be integrated into these programs. In order to achieve all of the above-mentioned requirements, the computers with high processor speeds are needed. More specifically,

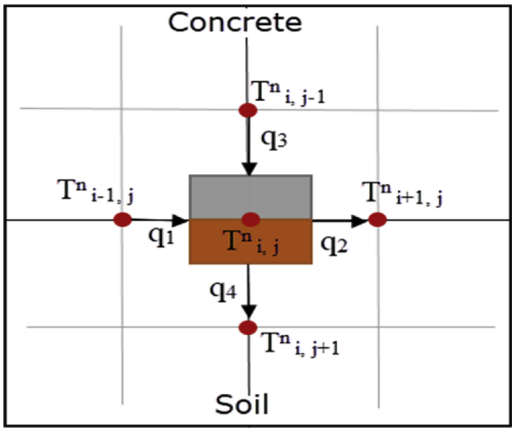

Fig. 6. Energy balance of soil and concrete interface.

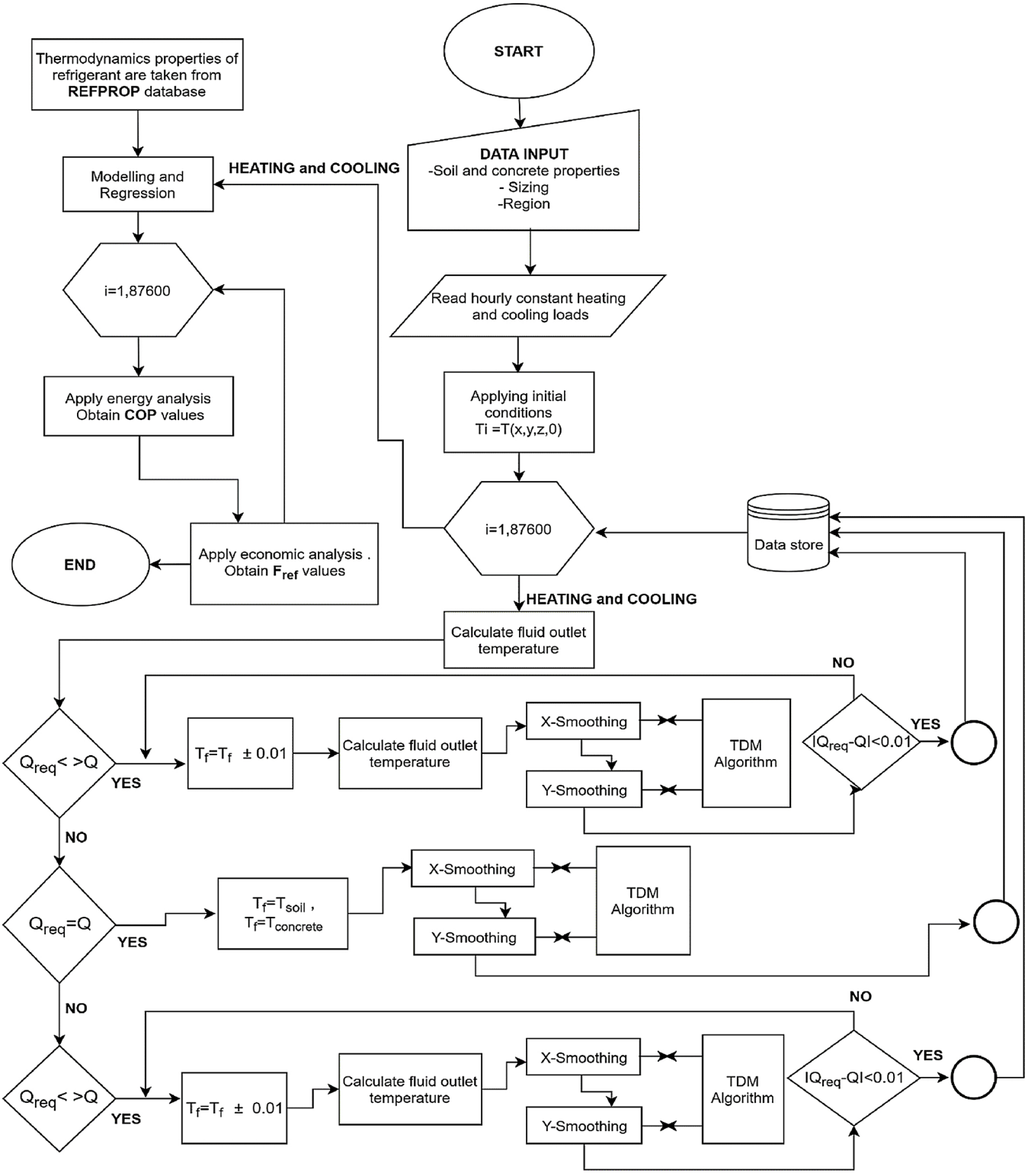

Fig. 7. Block diagram of solution algorithm.

using workstation class PC, one-year simulation for GHE design takes weeks in commercial programs while it takes days in the developed model. Therefore, the developed model allows the design of the GLHX with less computer power and less time.

The hourly fluid inlet and outlet temperatures in the pipe, soil and concrete temperatures around the pipe buried in the soil under the building foundation and in the building foundation are obtained for a ten-year period. By means of a new code developed in MATLAB, these temperatures are given as input parameters and then the energy analysis is performed in the heat pump cycle. By performing the energy analysis for all case studies, hourly COP values for ten years are calculated. Considering capital investment and operational costs, a reference function is defined as an optimization parameter. It is obtained for the all case studies.

4. Economical analysis and reference function

Capital investment costs of a GSHP system are as follows: pipe cost, earthwork cost, heat pump cost, circulation pump cost and labor cost. When the applications of GSHP systems are examined, the earthwork cost is the most important one among the capital investment costs. GSHP systems are generally implemented in the vicinity of buildings. The users avoid employing these systems due to higher costs of the excavation works compared to the conventional systems. Two methods are adopted to decrease or avoid the earthwork costs. Firstly, the earthwork cost is reduced by laying GLHX pipes in the soil under building foundation that is removed during the construction of the building. Secondly, the earthwork cost is eliminated by placing GLHX pipes in the building foundation during the construction.

Operational costs are also considerably indicative in the economic analysis of GSHP. As electricity prices, which vary according to fuel prices, increase, the costs of electric consumption in the compressor and pump increase, leading to an increase in operational costs. By means of a new code developed in MATLAB environment, the hourly COP values for 10 years are calculated as a result of the heat pump cycle analysis. The certain heating and cooling loads provided to shopping mall are divided into the hourly calculated COP values to obtain the electricity consumption of the compressor on hourly basis. The electricity consumption of the circulation pumps during the running time is also calculated. Following the total electricity consumption is calculated as specified, operational costs can be clearly determined.

The increase in electricity prices are added to these costs and the present values of the operational costs for each year are determined. Then, the capital investment costs are added to the present values of the operational costs. Taking into consideration the fact that Capital Recovery Factor (CRF) at a constant interest rate, the amount of total annual payment is determined. The reference function is determined by dividing the total annual heating and cooling loads provided to shopping mall into the total annual payment.

Capital investment costs of a GSHP system are as follows: pipe cost, earthwork cost, heat pump cost, circulation pump cost and labor cost. These costs of capital investment can be expressed as below:

$$C_i = C_{pipe} + C_{earthwork} + C_{heatpump} + C_{circpump} + C_{labor} \tag{35}$$

where C_i (ncu), the capital investment cost for yearly system operation. The general form of the cost functions of capital investment can be expressed as follows (Sanaye and Niroomand, 2010):

$$C_{pipe} = c_{pipe}(NPT)L_{GLHX} \tag{36}$$

$$C_{earthwork} = a_1 A_{earthwork} = a_1(NPT)L_{GLHX}(Y - Y_c) \tag{37}$$

$$C_{heatpump} = a_2 Q_{heatpump}^{a3} \tag{38}$$

$$C_{circpump} = a_4 W_{pump}^{a5} \tag{39}$$

c_{pipe} (ncu/m) is the regional cost of polyethylene pipe per meter depending on the geometrical properties of pipes. C_{labor} (ncu) is the total labor cost. It contains the piping between heat pumps and the places to be conditioned, the installation of heat exchanger pipes which is buried the soil under the building foundation and assembly and commissioning of heat pump. a_1 value is calculated according to the costs of earthwork and refilling. a_2–a_5 values are determined according to the load requirement to the shopping mall and regional price of the equipment.

The electricity consumption of GSHP systems are classified as follows: circulation pump and compressor. The electricity consumption of the circulating pump, E_{pump} (kWh), can be determined as below;

$$E_{pump} = (\tau_h + \tau_c)\frac{V_f H_{pump}}{\eta_{pump}} \tag{40}$$

where τ_h and τ_c (h) the total running hours in the heating and cooling season, respectively. By means of a new code developed in MATLAB environment, the hourly COP values for 10 years are calculated as a result of the heat pump cycle analysis. The certain heating and cooling loads provided to shopping mall are divided into the hourly calculated COP values to obtain the electricity consumption of the compressor, E_{comp} (kWh), on hourly basis. That is, it is obtained as shown below;

$$W_{comp,h} = \frac{Q_h}{COP_h},\ W_{comp,c} = \frac{Q_c}{COP_c} \tag{41}$$

$$E_{comp} = \sum W_{comp,h} + \sum W_{comp,c} \tag{42}$$

The total electricity consumption is calculated on an hourly basis and then operational costs, C_e (ncu), are obtained as follows:

$$C_e = (E_{pump} + E_{comp})E_{tariff} \tag{43}$$

where E_{tariff} (ncu/kWh), the tariff of unit electricity consumption of workplaces, which can be taken from ERRA. According to the ERRA of Turkey, the electricity prices for workplaces have gone up 11% in the last decade. This is called the increasing rates in electricity prices. Then, total cost of electricity consumption is obtained for a ten-year period as follows (Sullivan et al., 2008);

$$C_e = C_{e,1} + \sum_{n=2}^{n=10} C_{e,n}e \tag{44}$$

The increases in electricity prices, e, are added to these costs and the present values of the operational costs for each year are determined. Then, the capital investment costs are added to the present values of the operational costs. Taking into consideration the fact that Capital Recovery Factor (CRF) at a constant interest rate, the amount of total annual payment, A (ncu), is determined as below;

$$A = (C_i + C_e)CRF \tag{45}$$

where; CRF, is applied to distribute a single amount invested today over a uniform series of end year payments which have a present value equal to the amount invested today. It can be determined as follows;

$$CRF = \left[\frac{i(i+1)^y}{(i+1)^y - 1}\right] \tag{46}$$

The reference function, F_{ref} (kW/ncu), is determined by dividing the total annual heating and cooling loads provided to shopping mall into the total annual payment. It can be calculated as below;

$$F_{ref} = \frac{Q_h + Q_c}{A} \tag{47}$$

5. Experimental verification

The water inlet and outlet temperatures and flow rates were measured at every hour for 12 days. The input parameters (fluid, soil and pipe properties, pipe sizing and layout) of the experimental works for verification of the developed model are given below.

Experimental study started on 8th February 2018.

Soil and concrete thermal conductivity, k_s = 2 W/m K, k_c = 2.5 W/m K (ASHRAE Handbook, 1999).

Length of parallel pipes, L = 85 m.

Number of parallel pipes, NPT = 10.

Distance between pipes, P_s = 0.5 m.

Building foundation, Y_c = 1.30

Burial depth, Y = 1.45 m.

Working fluid = water.

Pipe material = HDPE.

Pipe thermal conductivity, k_p = 0.5 W/m K.

Pipe outer/inner diameter, do/di = 32/26 mm.

Mesh step in x and y direction, dx = dy = 0.05 m.

Mesh step along pipe axis, dz = 1 m, Time step, dt = 1800s.

As a result of experimental and simulation studies, the hourly variations of the experimental and numerical fluid inlet and outlet

temperature are given in Fig. 8. The fluid inlet temperature varies according to the required heating loads of occupied spaces. As the occupied space does not need the heating loads at the some time intervals, the system does not work.

As can be represented in Fig. 8a and b, the maximum difference between the measured and calculated hourly fluid inlet temperatures was obtained to be 1.45 °C whereas the maximum difference between the experimental and numerical hourly fluid outlet temperatures was found as 1.36 °C. Also, the maximum differences between the experimental and numerical daily average fluid inlet and outlet temperatures were found to be 1.09 °C and 0.84 °C respectively, as shown in Fig. 8c. In addition, the excess temperature projecting the temperature variation can be used to compare the experimental and simulation results, and the error can be expressed as follows;

$$\begin{pmatrix} \theta = T - T_{initial} \\ \theta' = T' - T_{initial} \end{pmatrix} \Rightarrow Error = (\theta - \theta')/\theta \tag{48}$$

where T is the experimental absolute temperature, T' is the numerical absolute temperature, $T_{initial}$ is the initial absolute temperature, θ is the excess temperature. The maximum errors between experimental and numerical hourly fluid inlet and fluid outlet temperatures were found to be 0.32 and 0.28. As can be clearly noted from Fig. 8a-c, the simulation results show good agreement with the experimental data.

The accuracy of the experimental study can be affected by the errors which may be caused for many reasons in the experimental study. Error in a measurement means the inevitable uncertainty that attends all measurements. Therefore, performing the error analysis is a very essential topic for experimental study. However, the error analysis is inherent in the measurement process and cannot be eliminated simply by repeating the experiment no matter how carefully. There are two different types of errors; bias (systematic) and random errors. Uncertainty analysis method, which is one of the most known and applied error analyses in the literature, is used in experimental study. The total error account can be calculated with the help of the following equation (Kline and McClintock, 1953);

$$W_R = \left[\left(\left(\frac{\partial R}{\partial x_1} w_1 \right) \right)^2 + \left(\left(\frac{\partial R}{\partial x_2} w_2 \right) \right)^2 + \ldots\ldots\ldots + \left(\left(\frac{\partial R}{\partial x_n} w_n \right) \right)^2 \right]^{1/2} \tag{49}$$

The error caused by thermocouples and PLC for temperature measurement is ± 0.3 °C and ± 0.2 °C, respectively. Also, the error caused by digital thermometer for calibration is ± 0.1 °C. The total error is calculated as below;

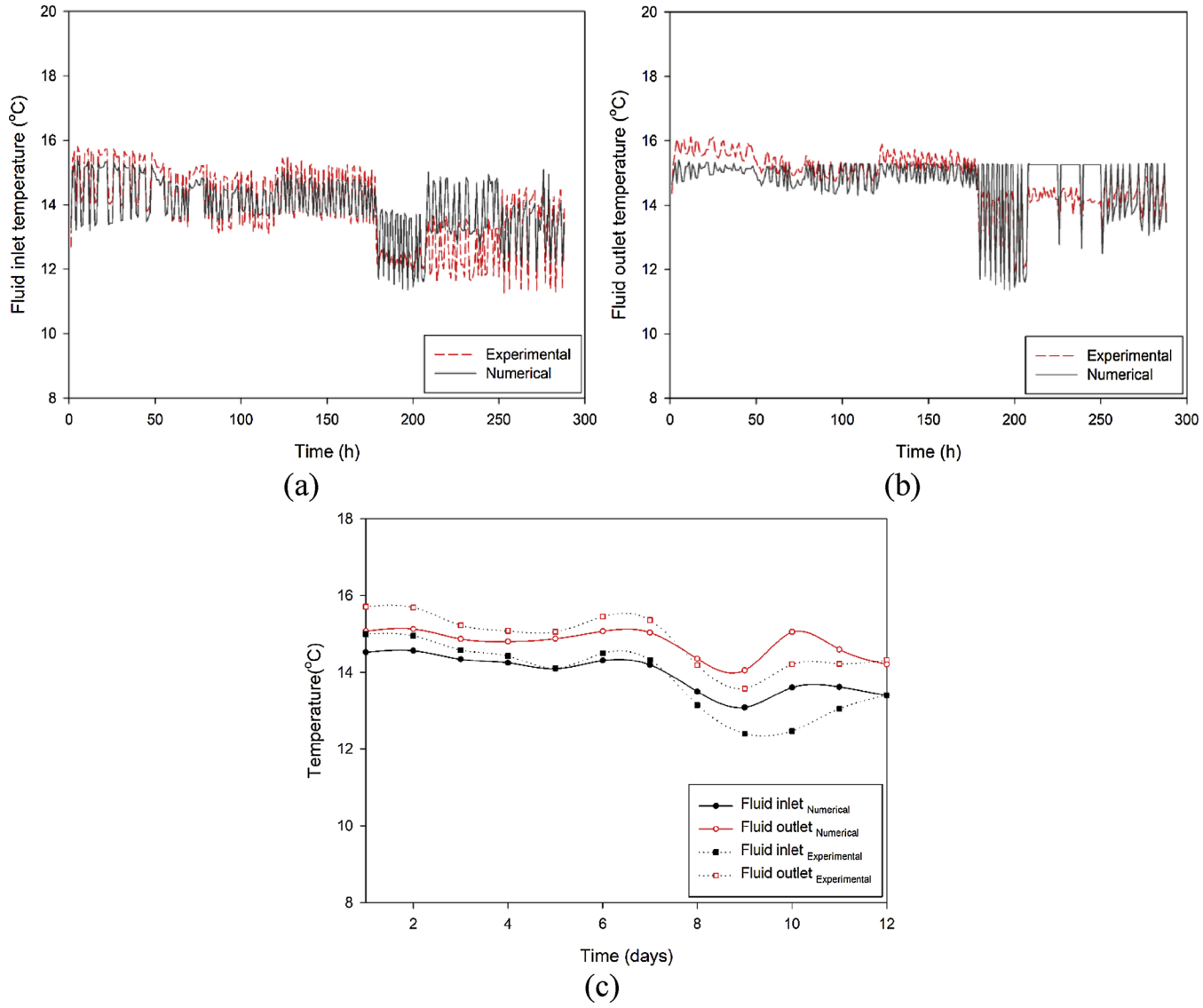

Fig. 8. Variations of hourly experimental and numerical (a) fluid inlet (b) fluid outlet temperatures, and daily average experimental and numerical fluid inlet and outlet temperature.

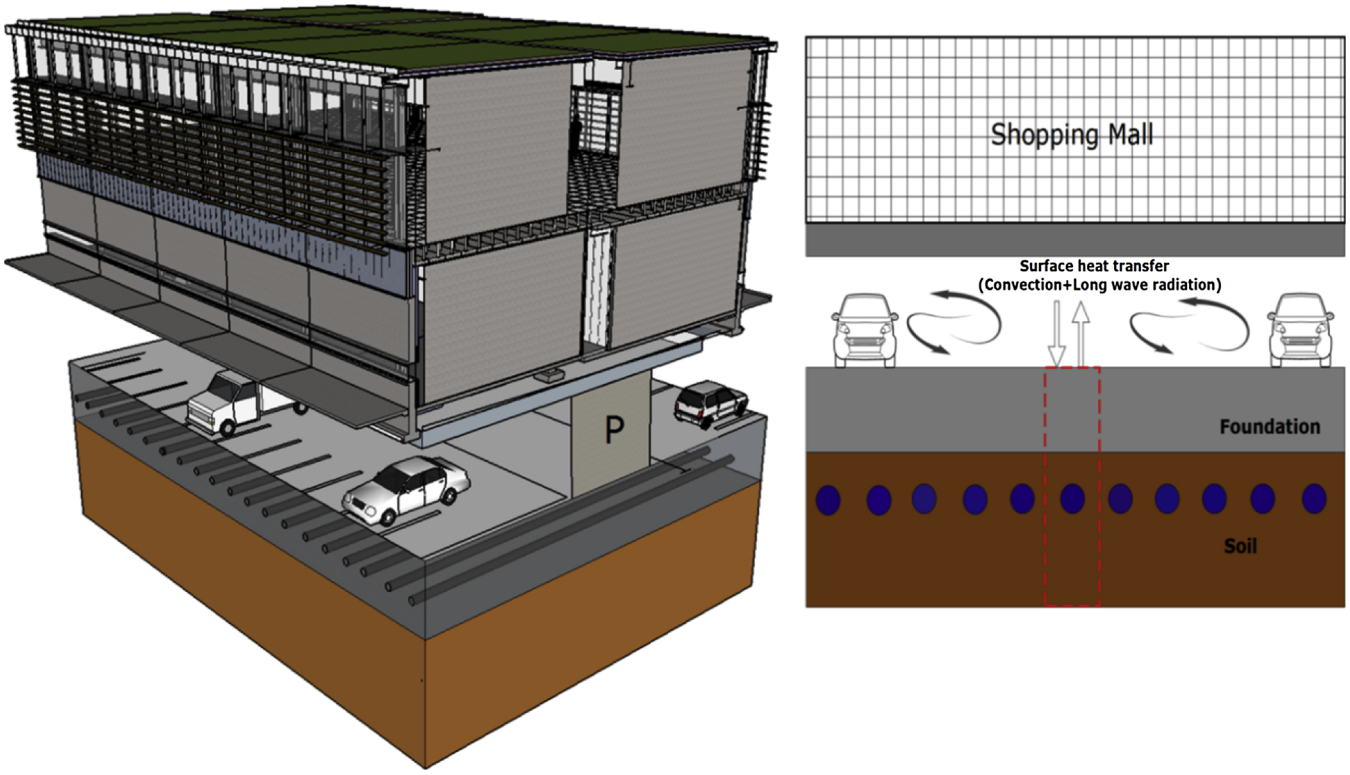

Fig. 9. Horizontal GLHX of the energy-foundation system.

Table 2
Conditions of all cases.

Cases	Installation place	Y-Y_c	Y	Y_c	NPT	T_{cond} in Heating season	T_{evap} in Cooling season	e
Case 1	Soil	0.2	–	0.75	30	30 °C	5 °C	8,
Case 2	Soil	0.2	–	0.75	40			10,
Case 3	Soil	0.2	–	0.75	50			12 %
Case 4	Soil	0.2	–	0.75	80			
Case 5	Soil	0.2	–	0.75	30	40 °C		
Case 6	Soil	0.2	–	0.75	40			
Case 7	Soil	0.2	–	0.75	50			
Case 8	Soil	0.2	–	0.75	80			
Case 9	Soil	0.2	–	0.75	30	50 °C		
Case 10	Soil	0.2	–	0.75	40			
Case 11	Soil	0.2	–	0.75	50			
Case 12	Soil	0.2	–	0.75	80			
Case 13	Concrete	–	0.8	1	30	30 °C		
Case 14	Concrete	–	0.8	1	40			
Case 15	Concrete	–	0.8	1	50			
Case 16	Concrete	–	0.8	1	80			
Case 17	Concrete	–	0.8	1	30	40 °C		
Case 18	Concrete	–	0.8	1	40			
Case 19	Concrete	–	0.8	1	50			
Case 20	Concrete	–	0.8	1	80			
Case 21	Concrete	–	0.8	1	30	50 °C		
Case 22	Concrete	–	0.8	1	40			
Case 23	Concrete	–	0.8	1	50			
Case 24	Concrete	–	0.8	1	80			

$$W_T = [(0.3)^2 + (0.1)^2 + (0.2)^2]^{1/2} = 0.374$$

As a result, the total error in temperature measurement is obtained as ± 0.374 °C.

The reading and processing error of turbine-type flow meter is ± 1%, the error is ± 0.01 m^3/h for a maximum measured flow rate of 1 m^3 / h. The accuracy of the turbine-type flow meter is ± 2 % and the error is ± 0.02 m^3 / h for a maximum measured flow rate of 1 m^3 / h. The total error is;

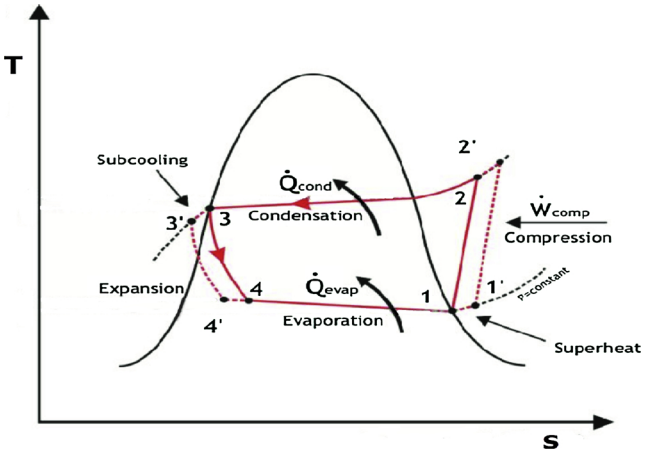

Fig. 10. T–s diagram of heat pump cycle.

Table 3
Points in the heat pump cycle.

Point	Inputs	Outputs
1	$T_1 = T_{evap} + T_{Superheating}$, $P_1 = P_{evap}$	h_1 and s_1
2	$P_2 = P_{cond}$, s_1	h_{2s}
	h_1, h_{2s}, $\eta_{comp,isen}$	$h_2 = h_1 + (h_{2s} - h_1)/\eta_{comp,isen}$
	P_2, h_2	s_2
3	$P_3 = P_2$, $T_3 = T_{3'} - T_{Subcooling}$,	s_3, h_3
4	$T_4 = T_{evap}$, $h_3 = h_4$	x_4, s_4

$$W_F = [(0.01)^2 + (0.02)^2]^{1/2} = 0.022$$

The total error in flow measurement is found as ± 0.022 m^3 / h."

When the living space does not need the heating load, the heat extracted from the Ground layer continues until the tank temperature reaches the operation temperature, and the heat pump switches itself

Table 4
Key parameters of case study.

Water, $V_{f,total}$ = 20 m^3/h	$T_{a,h}$ = 10 °C and $T_{a,c}$ = 20 °C
k_s = 2 W/m K, HDPE, k_p = 0.5 W/m K L = 40 m d_o/d_i = 32/26 mm	k_b = 2.5 W/m K P_s = 1 m H = 20 m Δx = Δy = 0.025 m, Δz = 1 m, Δt = 1800 s

Table 5
Critical parameters used in economic analysis.

$T_{cond,h}$ = 30 °C, 40 °C, 50 °C	$T_{evap,c}$ = 5 °C
$T_{evap,h}$ = ($T_{f,i}$ + $T_{f,o}$)/2 a_1 = 10 ncu/m^2 c_{pipe} = 2.1 ncu/m for DN32 $C_{heatpump}$ = 20,000 ncu e = 8, 10, 12% v = 10 year i = 12% $\eta_{pump,el}$ = 80%	$T_{cond,c}$ = ($T_{f,i}$ + $T_{f,o}$)/2 τ_h = 2310 h/y τ_c = 2800 h/y C_{labor} = (C_{ghe} + $C_{heatpump}$)*0.35 E_{tariff} = 0.43 ncu/kWh $\eta_{comp,isen}$ = 70% $\eta_{comp,el}$ = 80% $\eta_{pump,ise}$ = 80%

The unit ncu stands for the national currency unit.

off. Therefore, some deviations occur between the simulation results and the experimental data during this time intervals.

6. Case study

The GSHP system with horizontal GLHX provides great advantages in terms of cost-efficiency particularly when it is applied to a large area. Due to the significant population increase in Istanbul in recent years, many high-rise buildings and workplaces have been built and they mostly have underground car park. In these buildings, except for the applications of some vertical GSHP, horizontal GSHP has not been widely applied using energy-foundation systems yet. In horizontal parallel GSHPs applications, it is seen that the pipes of horizontal GLHX are generally buried in the gardens or surroundings of buildings. The increase in capital investment costs due to the excavation works makes the users avoid employing these systems in comparison with the conventional systems. In order to diminish or avoid the earthwork costs, two methods are adopted in this study. Firstly, the earthwork cost is reduced by placing the pipes of horizontal GLHX in the soil under the building foundation that is moved while the building is constructed.

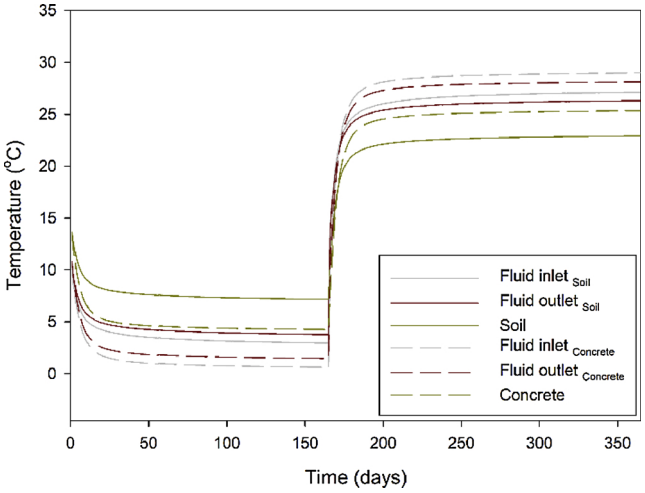

Fig. 12. Variation of daily average fluid inlet, outlet, soil and concrete temperatures for NPT = 50.

Secondly, the earthwork cost is eliminated by laying the pipes of horizontal GLHX in the building foundation during the construction. It is possible to diminish or avoid earthwork costs and to apply it into the building structure such as the underground car park.

Within the scope of numerical study, Fig. 9 shows the horizontal GLHX of the energy-foundation system placed in the soil under the building foundation and in the building foundation at the shopping mall with an underground car park.

An optimization study is carried out for the pipes of horizontal GLHX located in the soil under the foundation and in the foundation of a shopping mall with an underground car park, in Istanbul. The mall is conditioned from 9 a.m. till 10 pm all the year round. The system works for 14 h both in the heating and cooling season during the day throughout the year. It does not work in the rest of the day. In the heating and cooling season, during the time periods the system operates, a continuous 20 kW of total heating/cooling load of shopping mall is extracted/transferred from/to the soil or concrete. As the foundation is a covered space, the heat transfer with convection and long wave radiation takes place from the upper surface of the building foundation of the shopping mall with an underground car park. In case studies, the pipes of GLHX buried in the soil under the foundation and in the

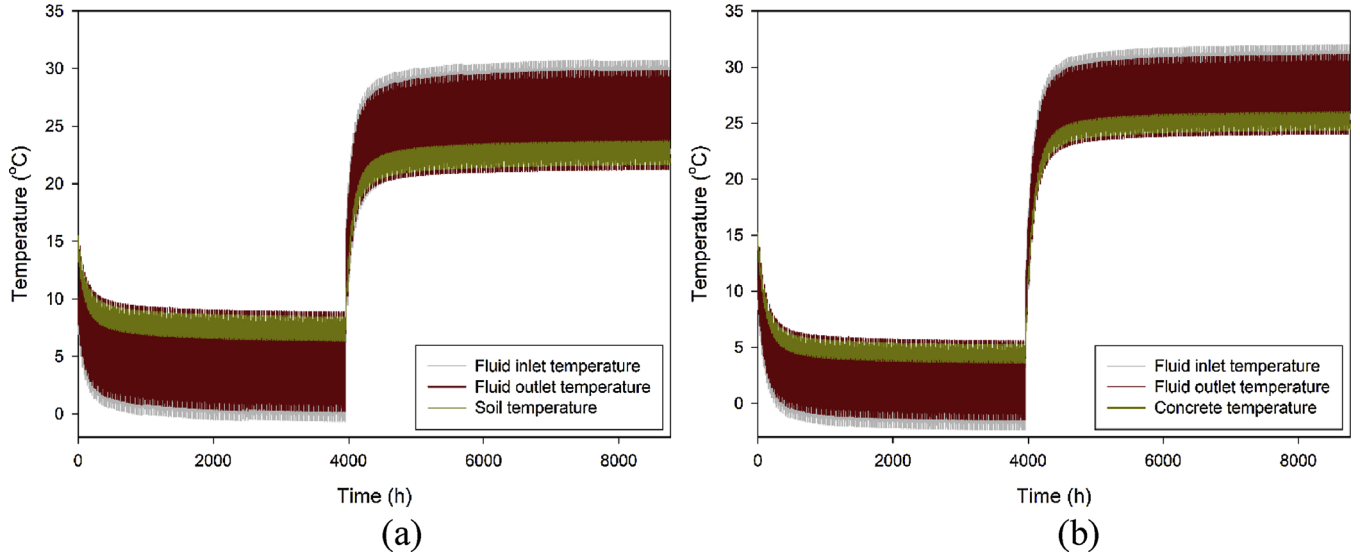

Fig. 11. Variation of fluid inlet, outlet, soil and concrete temperatures according to time if the pipes are buried (a) in soil under foundation of building and (b) in the foundation of building for NPT = 50.

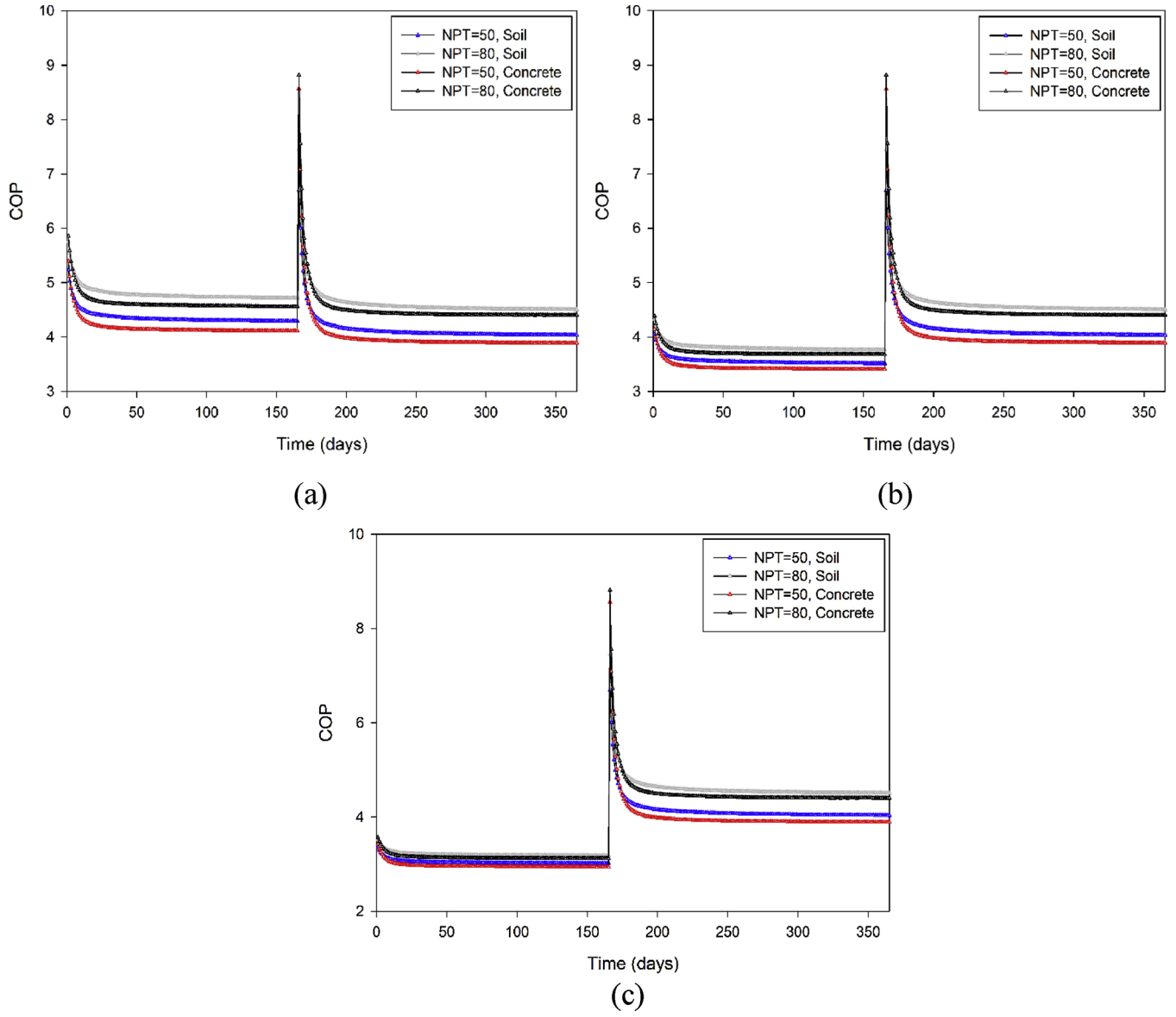

Fig. 13. The change of COP according to installation place of pipes and the number of different tubes for condensation temperature of (a) 30 °C, (b) 40 °C, (c) 50 °C.

foundation are examined for varied NPTs. Furthermore, several case studies are carried out by taking various condensation temperatures (30, 40, 50 °C) during the heating season and by taking a single evaporation temperature (5 °C) in the cooling season. In all the case studies, increase rates in the electricity prices are also taken into consideration. In summary, as seen in Table 2, case studies are conducted.

The analysis of the heat pump cycle is performed with a new code written in the MATLAB environment. T-s diagram of heat pump cycle and its details is displayed in Fig. 10. Principally, the hourly fluid inlet and outlet temperature in the pipe, soil and concrete temperatures vicinity of the pipe are obtained in ten years by conducting case studies. By means of a new code developed in MATLAB, these temperatures are given as input parameters and then the energy analysis is performed in the heat pump cycle. This procedure is carried out for 3 different condensation temperatures in the heating season. As a result of these optimization studies, many different case studies are obtained. By performing the energy analysis for all case studies, hourly COP values for ten years are calculated. The step-by-step determination of the thermodynamic properties of each point is given in Table 3.

In Table 4, the key input parameters used in case studies are given. It contains properties of fluid, soil and concrete, the placement of pipes and its thermal properties. The critical parameters used in economic analysis to obtain the reference function in all case studies are also listed in Table 5.

7. Results and discussion

The sizing of GLHX does not only depend on technical parameters, e.g. installation place of pipes, NPT and different condensation temperatures in the heating season but also on economic parameters such as capital, operation and maintenance costs, interest rate, electricity prices and its escalation rate. The hourly fluid inlet and outlet temperatures in the pipe, soil and concrete temperatures around the pipe laid in the soil under the building foundation and in building foundation were obtained for a period of ten years by conducting many case studies. The fluid inlet temperatures equivalent to the hourly need for the heating and cooling loads of the shopping mall all year round were simulated for a ten-year period in accordance with the different NPT and pipe location.

In Fig. 11, the variation of the fluid inlet, outlet, soil and concrete temperatures around the pipe according to time for the two different cases are given for a one-year period. The temperature profiles show

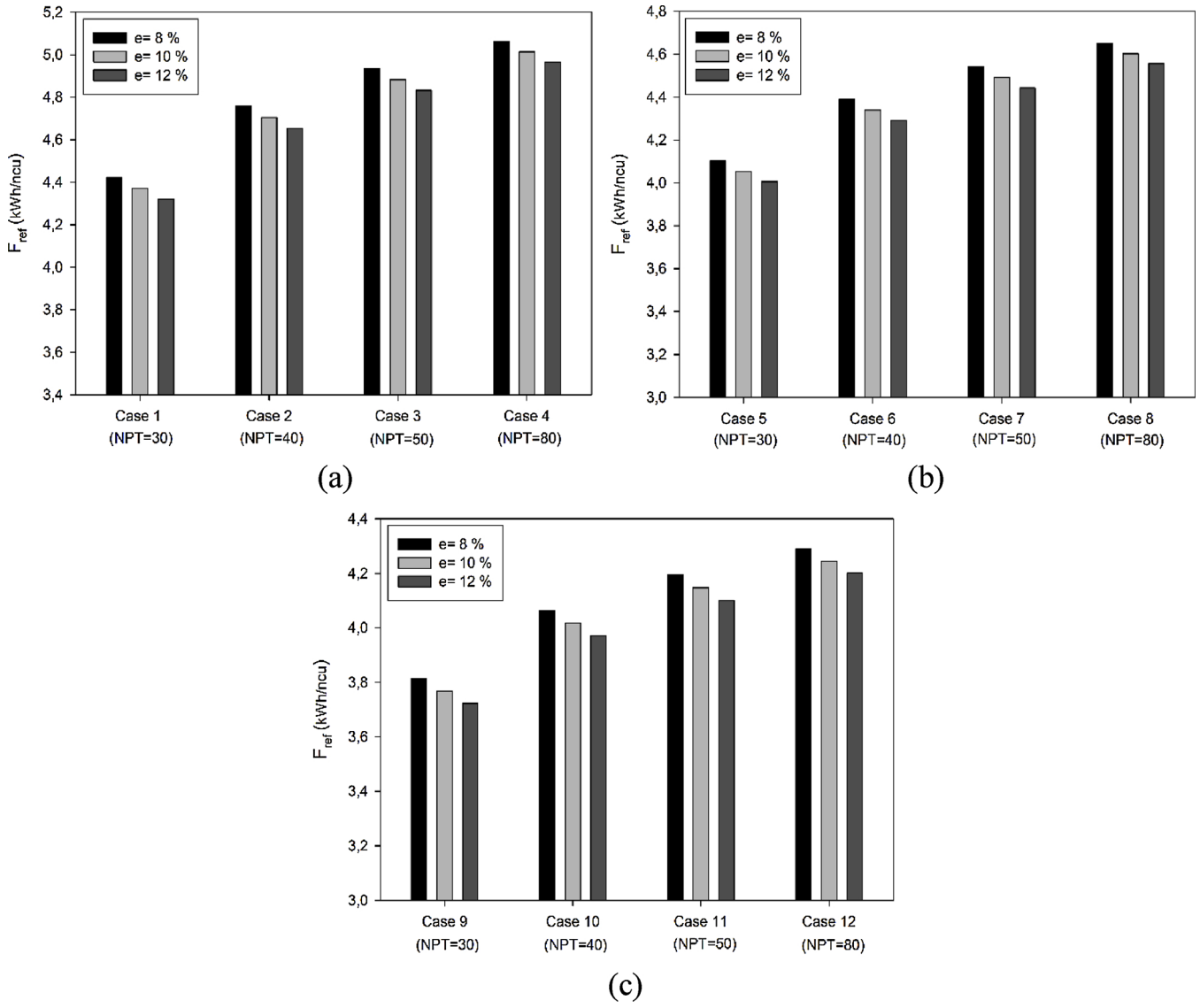

Fig. 14. Calculation results of all cases for condensation temperature of (a) 30 °C, (b) 40 °C.

similar trends for the heating and cooling seasons for both cases. The amplitude of the soil and concrete temperature is lower than the fluid inlet and outlet temperatures for a one-year period.

As shown in Fig. 11, the difference between amplitudes of the hourly soil and concrete temperatures is found approximately 2.5 °C. That is, the soil temperature is higher in heating season and lower in cooling season than concrete temperature. This result performs that the performance of GSHP systems is higher and the service life is longer. Besides, Fig. 12 shows the change of daily average fluid inlet, outlet, soil and concrete temperatures for NPT = 50. The fluid outlet temperature for the soil layer is higher during the heating season and lower during the cooling season compared to the concrete layer. In this case, it provides higher COP values of GSHP systems when the pipes are located in the soil.

In Fig. 13, the variation of COP values according to the installation place of the pipes and NPT for different condensation temperatures and evaporation temperature of 5 °C in heating and cooling seasons are given respectively. When the pipes are placed in the soil under the building foundation, the daily average COP_h and COP_c values are 4.78 and 4.62, whereas when the pipes are laid in the building foundation, the daily average COP_h and COP_c values are 4.62 and 4.52 for NPT = 80, T_{evap} = 5 °C and T_{cond} = 30 °C, respectively, as shown in Fig. 13a. It can be clearly seen that the daily average COP values are higher when the pipes are located in the soil for all three cases.

As represented in Fig. 13a and c, when the pipes are buried in the soil for condensation temperature of 30 °C in heating season, the daily average COP_h values are 4.35 and 4.78 for NPT = 50 and NPT = 80 respectively. Similarly, for condensation temperature of 50 °C in heating season, the daily average COP_h values are 3.03 and 3.20 for NPT = 50 and NPT = 80 respectively. It can be clearly expressed that the lower condensation temperatures are more suitable for GSHP. Therefore, using a GSHP system together with the wall panel heating system (T_{cond} = 30 °C), can be recommended. As can be clearly seen from Fig. 13a, when the pipes are buried in the soil, the daily average COP values at one year period are found to be 4.25 and 4.70 for NPT = 50 and NPT = 80 respectively. Therefore, it can be said that the placement of the pipes in the soil or the concrete, that is, in both cases, COP values increases as the NPT increases. Also, it is obviously noted that the COP values are highest for the beginning of the heating and cooling seasons due to the temperatures as a result of heat extraction/transfer during the both seasons (Fig. 13).

Considering the economic criteria, an optimization parameter is taken as the reference function defined above. In Figs. 14 and 15, the effects of NPT for the soil and concrete layers on reference function are

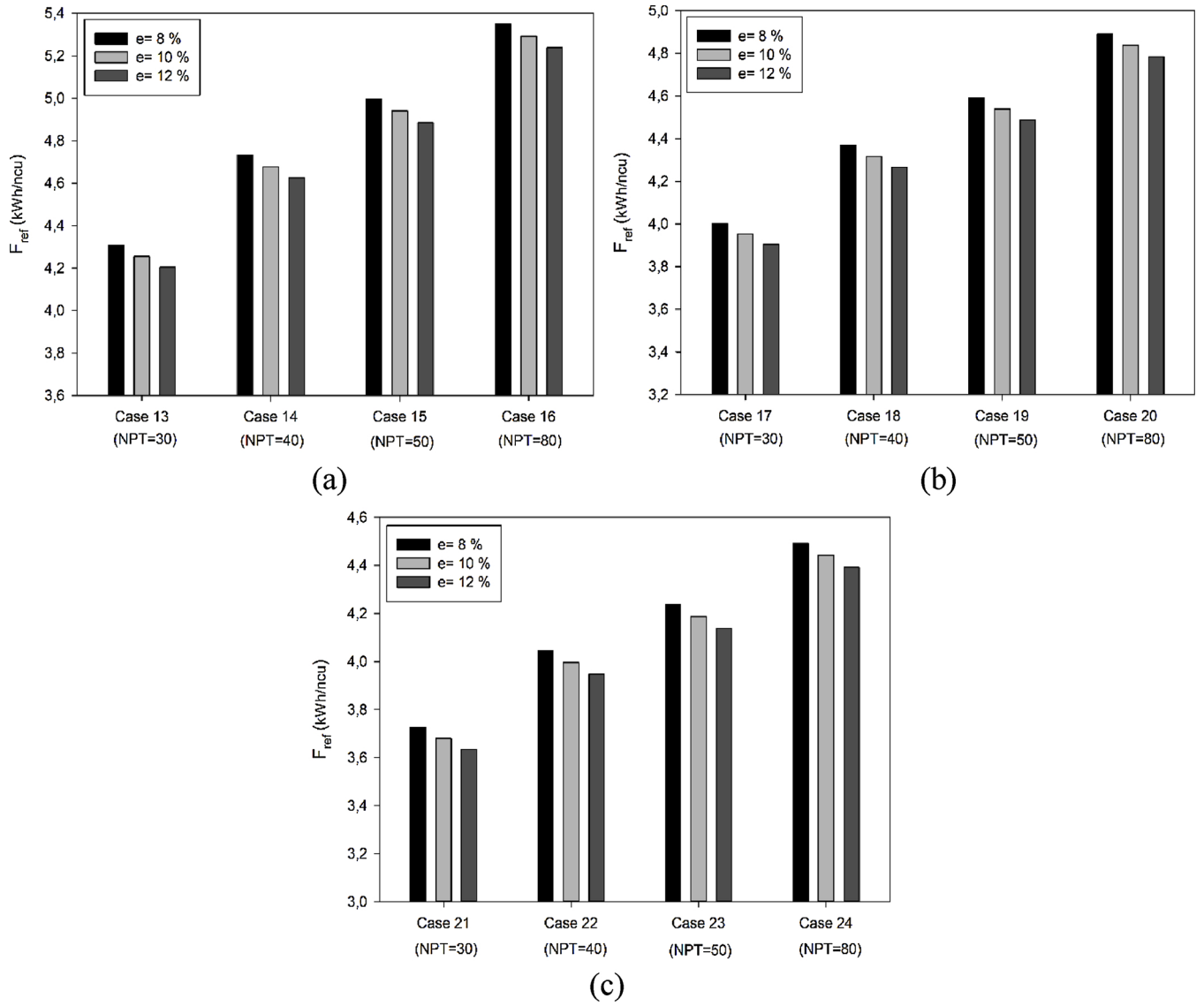

Fig. 15. Calculation results of all cases for condensation temperature of (a) 30 °C, (b) 40 °C, (c) 50 °C.

given together with the escalation rate in electricity prices for the condensation temperatures of 30, 40 and 50 °C (see in Table 2).

As can be clearly seen from Figs. 14 and 15, for NPT = 50, T_{cond} = 30 °C and the placement of pipes into the soil, the reference functions are found as 4.93, 4.88 and 4.83 at e = 8, 10 and 12 %, respectively. Reference function decreases as the escalation rate in electricity prices increases. For e = 8%, T_{cond} = 30 °C and NPT = 30, the reference functions are found to be 4.42 and 4.30 for soil and concrete layers respectively, while for e = 8%, T_{cond} = 30 °C and NPT = 80, the reference functions are obtained as 5.06 and 5.34 for the soil and concrete layers respectively. It can be expressly noted that increasing the NPT increases the reference function for both the soil and concrete layers.

As represented in 14a-c, for NPT = 40, e = 8% and the placement of pipes in the soil, the reference functions are obtained to be 4.75, 4.38 and 4.06 at condensation temperatures of 30 °C, 40 °C and 50 °C respectively. For NPT = 40, e = 8% and the placement of pipes in the concrete, the reference functions are found to be 4.73, 4.36 and 4.04 at condensation temperatures of 30 °C, 40 °C and 50 °C, respectively, as shown in 15a-c.

Likewise, for NPT = 50, e = 8% and the placement of pipes in the soil, the reference functions are obtained as 4.93, 4.54 and 4.19 at condensation temperatures of 30 °C, 40 °C and 50 °C respectively. For NPT = 50, e = 8% and the placement of pipes in the concrete, the reference functions are found as 4.99, 4.59 and 4.23 at condensation temperatures of 30 °C, 40 °C and 50 °C respectively. It can be clearly noted that while the reference function gives better results for the soil layer at NPT = 40, when NPT increases, it gives better results for concrete layer. Also, in Fig. 15a, it can be seen that the highest values of the reference function are achieved for Case 16 for condensation temperature of 30 °C together with the evaporation temperature of 5 °C. Installing the pipes of horizontal GLHX in the building foundation (concrete layer), earthwork costs will be eliminated. Therefore, higher values of the reference function are obtained.

Fig. 16a-c show the variations of the reference function according to NPT for soil and concrete layer at different condensation temperatures.

In Fig. 16, at the change of reference function obtained by considering technical and economic parameters, the intersection point of soil and concrete lines is very critical to decide where the pipes are buried. This is a breakpoint where the economic and technical parameters have equal importance. But when it is higher than NPT = 43, effects of economic parameters become dominant on the reference function. Therefore, the results performed that for higher NPT values (NPT > 43), locating the pipes in the building foundation (concrete

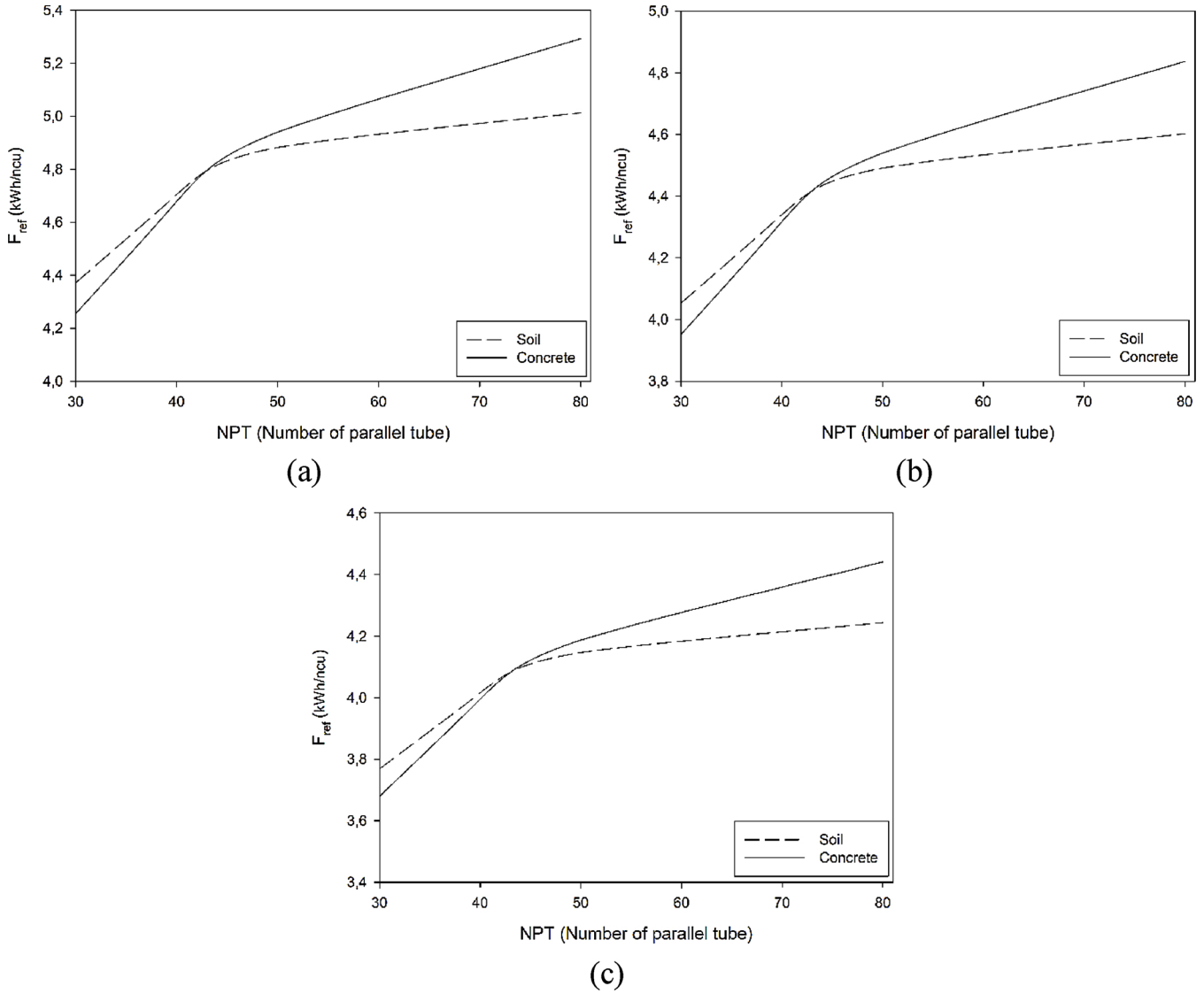

Fig. 16. The effects of NPT on the reference function for soil and concrete layer at condensation temperature of (a) 30 °C, (b) 40 °C, (c) 50 °C.

layer) gives higher values of the reference function while for lower NPT values it is vice versa.

8. Conclusions

In this study, firstly, experimental studies were performed on horizontal GLHX pipes buried in soil under the foundation of the 2400 m^2 Central Laboratory building newly established at Yıldız Technical University and the newly developed numerical model was validated with experimental results. The maximum percent differences between the experimental and numerical daily average fluid inlet and outlet temperatures were found to be 8.36% and 5.58%, respectively (Fig. 8c). The simulation results performed good agreement with experimental data. Then, the hourly simulations of a shopping mall were conducted for a period of ten years. The variation of the fluid inlet and outlet temperatures as well as the soil or concrete temperatures were obtained. The effects of pipe location (soil or concrete layers) and NPT on the soil and concrete temperature were investigated. According to the obtained fluid and soil or concrete temperatures, hourly COP values and energy consumptions were calculated with a new code developed in MATLAB environment.

A reference function including economic and technical parameters was defined and investigated for different cases. Following conclusions were achieved:

- The results obtained from the experimental work were confirmed by numerical study and found to be very compatible.
- Hourly COP values were calculated according to obtained fluid and soil or concrete temperatures for a ten-year period and used in simulations and economic analysis as well.
- Higher COP values for all the simulations were obtained when the pipes are located in the soil. Also, it can be said that when the pipes are placed in the soil or the concrete, that is, in both cases, COP values increases as the NPT increases (Fig. 13).
- Rate of increase in electricity prices has negative effect on reference function.
- Lower condensation temperatures are more suitable for GSHP. Therefore, using a GSHP system together with the wall panel heating system is suggested.
- Increasing the NPT increases the reference function for both soil and concrete layers (Figs. 14 and 15).
- To ensure the highest performance of a GSHP system, a complete analysis considering all technical and economical parameters should be done for minimum ten years period. Case 4 ($Y\text{-}Y_c$ = 0.2 m, Y_c = 0.75 m, NPT = 80, T_{cond} = 30 °C and e = 8%) and Case 16 (Y = 0.8 m, Y_c = 1 m, NPT = 80, T_{cond} = 30 °C and e = 8%) gave

the best results when the heat exchanger pipes are buried in the soil under the building foundation and in the building foundation, respectively. However, for higher NPT values (NPT > 43), locating the pipes in the building foundation (concrete layer) was obtained higher values of reference function while for lower NPT values it is vice versa (Fig. 16).

It is concluded that by means of GLHX and GSHP simulation code developed in MATLAB environment, every GSHP system can be investigated individually and optimum design conditions can be obtained based on meteorological data, and technical and economic parameters as well.

Declaration of Competing Interest

The authors declare that they have no known competing financial interests or personal relationships that could have appeared to influence the work reported in this paper.

Acknowledgements

The authors gratefully acknowledge the financial support from Ministry of Science, Industry and Technology of Turkey and Mir Unique Solutions (No. 0472.STZ.2013-2) for this study performed.

References

ASHRAE Geothermal heating and cooling, 2014. Design of Ground-source Heat Pump Systems.
ASHRAE Handbook. Appendix B Materials References.
Chiasson, A.D., 1999. Advances in Modeling of Ground Source Heat Pump Systems, MSc Thesis. Oklahoma State University.
Demir, H., Koyun, A., Temir, G., 2009. Heat transfer of horizontal parallel pipe ground heat exchanger and experimental verification. Appl. Therm. Eng. 29, 224–233.
Gu, Y., O'Neal, D.L., 1995. An analytical solution to transient heat conduction in a composite region with a cylindrical heat source. Trans. ASME 117, 242–248.
Hastaoglu, M.A., Negiz, A., Heidemann, R.A., 1995. Three-dimensional transient heat transfer from a buried pipe – part III comprehensive model. Chem. Eng. Sci. 50, 2545–2555.
Kasuda, T., Archenbach, P.R., 1965. Earth temperature and thermal diffusivity at selected stations in the United States. ASHRAE Trans. 71 Part 1.
Kayaci, N., Demir, H., 2018a. Numerical modelling of transient soil temperature distribution for horizontal ground heat exchanger of ground source heat pump. Geothermics 73, 33–47.
Kayaci, N., Demir, H., 2018b. Long time performance analysis of ground source heat pump for space heating and cooling applications based on thermo-economic optimization criteria. Energy and Building 163, 121–139.
Kayaci, N., Demir, H., Kanbur, B.B., Atayilmaz, O., Ağra, O., Acet, R.C., Gemici, Z., 2019. Experimental and numerical investigation of ground heat exchangers in the building foundation. Energy Convers. Manage. 188, 162–176.
Kline, S.J., McClintock, F.A., 1953. Describing the uncertainties in single sample experiments. Mech. Eng. 3–8.
Lei, T.K., 1993. Development of a computational model for a ground-coupled heat exchanger. ASHRAE Trans. Res. 99, 149–159.
Ling, F., Zhang, T., 2004. A numerical model for surface energy balance and thermal regime of the active layer and permafrost containing unfrozen water. Cold Reg. Sci. Technol. 38, 1–15.
Lund, J.W., Boyd, T.L., 2015. Direct utilization of geothermal energy 2015 worldwide review. Proceedings World Geothermal Congress.
Mei, V.C., 1991. Heat transfer of buried pipe for heat pump application. J. Solar Energy Eng. 113, 51–55.
Metz, P.D., 1983. A Simple computer program to model three-dimensional underground heat flow with realistic boundary conditions. Trans. ASME 105, 42–49.
Mihalakakou, G., 2002. On estimating soil surface temperature profiles. Energy Build. 34, 251–259.
Moon, C.E., Choi, J.M., 2015. Heating performance characteristics of the ground source heat pump system with energy-piles and energy-slabs. Energy 81, 27–32.
Mukerji, S., Tagavi, K.A., Murphy, W.E., 1997. Steady-state heat transfer analysis of arbitrary coiled buried pipes. J. Thermophys. Heat Transf. 11, 182–188.
Nam, Y., Chae, H.B., 2014. Numerical simulation for the optimum design of ground source heat pump system using building foundation as horizontal heat exchanger. Energy 73, 933–942.
Negiz, A., Hastaoglu, M.A., Heidemann, R.A., 1993. Three-dimensional heat transfer from a buried pipe – I. Laminar flow. Chem. Eng. Sci. 48, 3507–3517.
Negiz, A., Hastaoglu, M.A., Heidemann, R.A., 1995. Three-dimensional transient heat transfer from a buried pipe: solidification of a stationary fluid. Numer. Heat Transf. 28, 175–193.
Rezaei, A., Kolahdouz, E.M., Dargush, G.F., Weber, A.S., 2012. Ground source heat pump pipe performance with Tire Derived Aggregate. Int. J. Heat Mass Transf. 55, 2844–2853.
Sanaye, S., Niroomand, B., 2010. Horizontal ground coupled heat pump: thermal-economic modeling and optimization. Energy Convers. Manage. 51, 2600–2612.
Sullivan, W.G., Wicks, E.M., Koelling, C.P., 2008. Engineering Economy. Pearson Education.
Von Rosenberg, D.U., 1969. Methods for the Numerical Solution of Partial Differential Equations. Publishing Division Gerald L. Farrar & Associates Inc., Tulsa.